A Numerical Model of the Synthesis of Carbon Black by Benzene Pyrolysis

A numerical model has been developed to predict the formation of carbon black particles by benzene pyrolysis. The approach, patterned after the work of Jensen, assumes that particle formation is controlled by four steps: gas phase reactions producing radical species, nucleation, growth and coagulation, and oxidation. In the present model, 15 reactions based on the work of Fujii and Asaba are used to describe the gas phase kinetics in which the phenyl radical is treated as the important intermediate in the formation of carbon black. A discrete distribution of 10 particle radii is also used to approximate the simultaneous growth and coagulation of spherical carbon particles. The results of the model show that a self-preserving log normal distribution of carbon particles develops after an initial nucleation and growth period. The model results also compare favorably with reactor data. In particular, the numerical model predicts a mass median carbon particle diameter to within 10% of measured values.

J. J. Ivie, L. J. Forney
School of Chemical Engineering
Georgia Institute of Technology
Atlanta, GA 30332-0100

Introduction

Carbon black is a form of amorphous carbon produced from the partial oxidation and/or thermal decomposition of hydrocarbon gases or liquids. The reactions that occur form extremely small, finely divided carbon particles of an intense black color. Unlike other carbon-forming reactions that produce coke and char from the pyrolysis of solids, carbon black is formed in the vapor phase surrounding a flame. When the carbon particles are filtered from the vapor phase, a fluffy black powder is obtained that can be identified by its chemical composition, pigment properties, state of subdivision, and other colloidal properties.

The purpose of the present study is to propose a numerical model that simulates the formation of the carbon particles in a carbon black reactor. In the model the carbon particles are formed in a four-step process:

1. Formation of the gaseous radical species (preparticle kinetics)
2. Nucleation of the carbon particles
3. Growth on and coagulation among the carbon particles
4. Oxidation of the carbon particles (burnout)

Figure 1 shows the section of the reactor simulated by the model. Vaporized feedstock (benzene) is burned and pyrolyzed to form gaseous radials which then form the nuclei of the carbon particles. These preparticle nuclei subsequently grow into particles by coagulating with other radical molecules that act as growth species. Also, particles are allowed to coagulate with one another to form larger individual particles and agglomerates. Finally, oxidizing species such as hydroxyl radicals (OH) may attack the carbon particles, causing either partial or total oxidation of the carbon particles.

In the present model the reactor is considered to be an isothermal, homogeneously mixed plug flow reactor. Incomplete mixing between the combustion gas stream and the feedstock that may occur and affect the carbon formation within the reactor has been neglected (Donnet and Voet, 1976). Moreover, the nonspherical nature of the particles is neglected although carbon black particles are known to consist of primary spherical nodules grouped together in agglomerates (Medalia, 1967).

In this paper the technique used to model each of the steps in the particle formation is described. Also, the results from the model are discussed and compared with pilot plant data taken from an operating reactor.

Theory

Preparticle kinetics

The first step in the formation of the carbon particles is the creation of important molecular precusor species from the oil feedstock. To simplify the analysis of the thermal decomposition

Correspondence concerning this paper should be addressed to L. J. Forney.

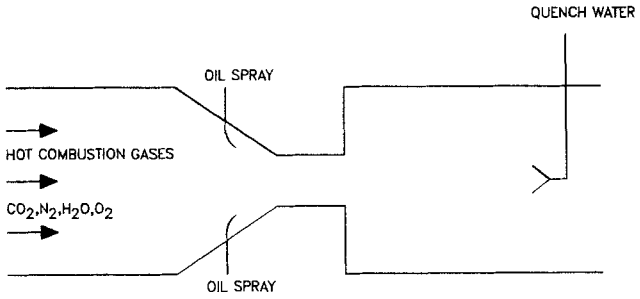

Figure 1. A carbon black reactor.

and oxidation of the oil feedstock, benzene has been substituted for the feedstock oil in the present study. The feedstock oil normally used is a heavy aromatic oil that originates from the bottoms of a fractionation column. Because of the similarities in the carbon-to-hydrogen ratio and the aromaticity, experimental results are insensitive to the use of either the feedstock oil or benzene in the carbon-forming process (personal communication, P. J. Cheng, Phillips Petroleum Co., 1985).

Several mechanisms have been proposed to predict the important precusors in carbon black particle formation (Graham et al., 1975; Howard and Bittner, 1980; Lahaye and Prado, 1978; Palmer and Cullis, 1965; Haynes and Wagner, 1981). The model of Abrahamson (1977), however, is chosen as the basis for the present study. In Abrahamson's model the phenyl radical C_6H_5 is treated as the important intermediate. Here, acetylene and other carbon species formed from a ring-fracturing reaction attach onto phenyl radicals, forming networks of aromatic rings as shown in Figure 2. These growing aromatic ring structures act as the initial nuclei for the carbon particles. Abrahamson's model is supported by the fact that aromatic fuels have a greater tendency to produce carbon particles at lower fuel/air ratios. Since the phenyl radical is initially present in an aromatic fuel, formation reactions are bypassed. Also, Abrahamson found that young soot particles have a C/H ratio <2, corresponding to the C/H ratio in the growing ring structures. As the carbon particles age, dehydrogeneration occurs so that the final C/H ratio in carbon black particles is approximately 10.

A competition occurs between the thermal decomposition of

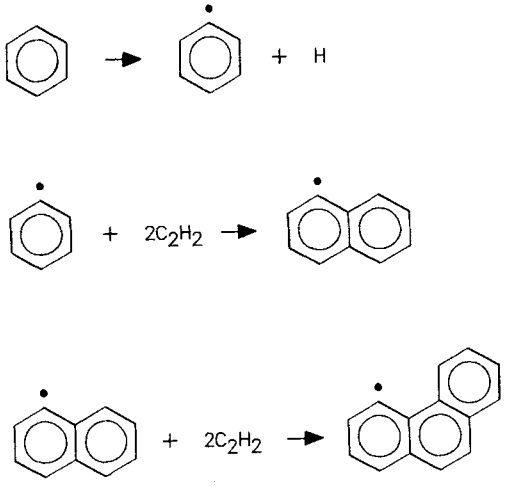

Figure 2. Abrahamson's mechanism for initial nucleation of carbon black particles.

the oil (benzene) and oxidation reactions in the reactor. In the combustion gas stream enough residual oxygen is present to burn 5 to 20% of the oil. The oil combustion is necessary to attain temperatures high enough for the pyrolytic reactions to occur. Therefore, both pyrolytic and oxidation reactions are accounted for in the gas phase kinetics.

Table 1 shows the pyrolytic reactions used in the present model and their rate constants. Reactions 1 through 11 shown in Table 1 were taken from a shock tube study by Fujii and Asaba (1977). In their study benzene and oxygen mixtures were studied at temperatures and concentrations comparable to the conditions found in a carbon black reactor. Several of the rate constants determined by Fujii and Asaba have been replaced in Table 1 with the referenced updated values.

As shown by the reaction scheme in Table 1, phenyl radicals are produced along with the ring fracture products (C_2H_2, C_2H_3, C_4H_3) suggested by Abrahamson's theory. In the oxidation reactions also shown in Table 1, some of the phenyl radicals are lost in reaction 11 where oxidation occurs, resulting in the formation of carbon monoxide. Not all of the carbon is lost to oxidation products in reaction 11, however, since the products of ring-fracturing cause carbon particle growth.

Nucleation

After the particle precusors are formed, the growth molecules begin colliding and sticking onto the precusors. In an approach similar to that of Jensen (1974), a particle is considered to be formed when enough growth onto the precursor has occurred. In Jensen's model, however, acetylene is considered to be the initial building block of soot particles. Because Jensen is modeling soot formation from methane pyrolysis, phenyl radicals are not available in his study for nucleation and a carbon particle is formed when two aceytlenes collide, forming an initial particle with four carbon atoms.

Because of the availability of phenyl radicals and biphenyl molecules during the pyrolysis of benzene in the present study, these species are now considered to be the initial nuclei of the carbon particles. In the present model the assumption is made that a particle is formed when a biphenyl or phenyl radical grows to contain 14 carbon atoms. The nucleation reaction would then take the form:

$$Ny + nGx \rightarrow Pz \qquad (1)$$

where Ny = nucleating species containing y carbon atoms (C_6H_5 or $C_{12}H_{10}$)
Gx = growth species containing x carbon atoms (C_2H_2, C_2H_3, or C_4H_3)
Pz = particle containing $z = 14$ carbon atoms
$n = (z - y)/x$

For example, four acetylenes must collide with a phenyl radical before a particle is formed. Other possible combinations that will form initial particles with 14 carbon atoms are one acetylene colliding with a biphenyl radical or two diacetylenes (C_4H_3) colliding with a phenyl radical.

Growth and coagulation

Once particles are formed, collisions between two different particles will occur, causing growth in particle size. In addition

Table 1. Gas Phase Reactions

	A cm³/mol · s	E kJ	Ref.
Pyrolysis Reactions			
1. $C_6H_6 \rightarrow C_6H_5 + H$	5.0×10^{15}	452	Hsu et al. (1984)
2a. $C_6H_6 + H \rightarrow C_6H_5 + H_2$	2.5×10^{11}	67	Kiefer et al. (1985)
2b. $C_6H_5 + H_2 \rightarrow C_6H_6 + H$	3.1×10^{09}	71	Kiefer et al. (1985)
3a. $C_6H_6 + C_6H_5 \rightarrow C_{12}H_{10} + H$	4.0×10^{09}	50	Singh & Kern (1983)
3b. $C_{12}H_{10} + H \rightarrow C_6H_6 + C_6H_5$	1.3×10^{13}	13	Fujii & Asaba (1977)
4a. $C_{12}H_{10} \rightarrow 2C_6H_5$	7.9×10^{14}	0	Fujii & Asaba (1977)
4b. $2C_6H_5 \rightarrow C_{12}H_{10}$	1.3×10^{4}	0	Fujii & Asaba (1977)
5. $C_6H_5 \rightarrow C_2H_2 + C_4H_3$	1.6×10^{12}	343	Kiefer et al. (1985)
Oxidation Reactions			
6. $C_6H_6 + O_2 \rightarrow C_6H_5 + HO_2$	6.3×10^{10}	251	Fujii & Asaba (1977)
7. $C_6H_6 + O \rightarrow C_6H_5 + OH$	3.2×10^{11}	25	Fuji & Asaba (1977)
8. $C_6H_6 + OH \rightarrow C_6H_5 + H_2O$	2.1×10^{10}	19	Madronich & Felder (1985)
9. $C_6H_6 + HO_2 \rightarrow C_6H_5 + H_2O_2$	1.0×10^{08}	76	Fujii & Asaba (1977)
10. $H + O_2 \rightarrow OH + O$	2.2×10^{11}	70	Frenklach & Warnatz (1987)
11. $C_6H_5 + O_2 \rightarrow 2CO + C_2H_2 + C_2H_3$	1.0×10^{09}	8	Fujii & Asaba (1977)
12. $C_X + OH \rightarrow C_{X-1} + CO + H$	1.9×10^{12}	34	Fenimore & Jones (1967)

to coagulation, growth of the particle also proceeds by continued adsorption of the growth molecules by the particle.

To model the growth and coagulation of an aerosol system, three approaches are available (Seigneur et al., 1986). The basic difference between the models is the manner in which the particle distributions are represented. Either a continuous, a discrete (sectional), or a parametrized (e.g., log normal) representation may be used to represent the size distribution of particles. The discrete distribution is used in the present model because no predetermined size distribution is assumed as it is in the parameterized representation. Also, the inherent inaccuracies in the preparticle kinetics do not warrant the use of the continuous representation, which is more computationally intensive than the discrete method.

As in the work of Jensen (1974), discrete particle classes have been chosen to follow the coagulation and growth of the particles once they have been formed. Table 2 shows the 10 discrete particle classes used in the present study and their characteristics. Similar to the results of Gelbard et al. (1980), 10 particle classes were found to adequately approximate the particle distribution. The spacing of the particle classes was specified so that particles can only coagulate and grow into adjacent size classes. This method of spacing simplified coding and implementation of the coagulation and growth equations in the model.

For the particles, 10 equations (one for each particle class) are used to relate the growth and coagulation of particles from one class to the next. Each of these equations relates the rate of change in concentration of one of the particle classes to the concentrations of all classes. The particle equations are similar to the molecular species equations. The growth and coagulation of particles can thus be thought of as a chemical reaction that takes the form:

$$Py + nPx \rightarrow Pz \tag{2}$$

where Py = particles with y carbon atoms
Px = particles with x carbon atoms
Pz = particles with z carbon atoms
$n = (z - y)/x$

The equations describing the growth and coagulation symbolized by Eq. 2 are:

$$d[Px]/dt = -fxy[Px][Py] \tag{3}$$

$$d[Py]/dt = -fxy[Px][Py]/n \tag{4}$$

$$d[Pz]/dt = fxy[Px][Py]/n \tag{5}$$

where fxy = coagulation rate constant for the particle in size class x and y.

Each rate equation for the particle classes used in the model relates the addition and loss of particles to that specific size class. For example, in Table 2 there are four ways in which particles can grow into the D size class:

1. $Pc + n$ growth molecules $\rightarrow Pd$
2. $Pc + 337\ Pa \rightarrow Pd$
3. $Pc + 94\ Pb \rightarrow Pd$
4. $Pc + 13\ Pc \rightarrow Pd$

In addition, there are 10 ways in which particles are lost from the D class when they coagulate with other particles:

1. $Pd + n$ growth molecules $\rightarrow Pe$
2. $Pd + 5{,}209\ Pa \rightarrow Pe$
3. $Pd + 1{,}458\ Pb \rightarrow Pe$
4. $Pd + 203\ Pc \rightarrow Pe$
5. $Pd + 14\ Pd \rightarrow Pe$
6. $Pe + 268\ Pd \rightarrow Pf$

Table 2. Characteristics of Discrete Particle Size Classes

Class	No. of C Atoms	Particle Dia. nm
A	14	0.64
B	50	0.98
C	360	1.90
D	5,080	4.60
E	7.80×10^{4}	11.0
F	1.44×10^{6}	30.0
G	1.32×10^{7}	64.0
H	1.06×10^{8}	130.0
I	1.47×10^{9}	300.0
J	2.32×10^{10}	760.0

7. $Pf + 2{,}315\ Pd \rightarrow Pg$
8. $Pg + 18{,}268\ Pd \rightarrow Ph$
9. $Ph + 268{,}504\ Pd \rightarrow Pi$
10. $Pi + 4{,}277{,}559\ Pd \rightarrow Pj$

Therefore, the equation describing the loss and addition of particles to the D size class contains 14 terms (four addition and 10 loss terms).

Every interaction between particles of two size classes has a coagulation constant fxy that predicts the number of collisions that occur between particles of the particular size classes. These coagulation rate constants are similar to the rate constants of chemical reactions. They relate the rate of change in concentration of a particular size class to the concentrations of the other size classes. Because of the variation in particle size in Table 2, the coagulation rate constants for the particles must apply to both small particles with large Knudsen numbers (free molecular Brownian coagulation) and large particles with small Knudsen numbers (continumum Brownian coagulation). Fuchs (1964) derived an expression that fits the coagulation coefficients for both regimes as shown below:

$$fxy = 4\pi(D_x + D_y)(r_x + r_y) \cdot \left[\frac{r_x + r_y}{r_x + r_y + g_{xy}} + \frac{4(D_x + D_y)}{(C_x^2 + C_y^2)^{1/2}(r_x + r_y)}\right]^{-1}$$

where D_i = diffusion coefficient of particle i
r_i = radius of particle i
C_i = mean thermal velocity of particle i
l_i = mean free path of particle i $(8D_i/\pi C_i)$
$g_i = (1/6r_i l_i)[(2r_i + l_i)^3 - (4r_i^2 + l_i^2)^{3/2}] - 2r_i$
$g_{ij} = [g_i^2 + g_j^2]^{1/2}$

Fuch's expression is used in the model to calculate the Brownian coagulation constants for each particle class interaction. For simplicity, it is also assumed in the present model that the carbon particles are spherical and that they stick together upon collision. Moreover, coagulation of the particles by turbulent shear was found to be insignificant compared to the Brownian coagulation mechanism.

Burnout

Reaction 12 in Table 1 accounts for carbon particle burnout in the model. After the carbon particles are formed, oxidation species such as hydroxyl radicals (OH) attack the carbon particle and cause the oxidation of one of the carbon atoms from the particle. The process causes a shrinkage of the carbon particle or even total elimination of the particle if enough oxidation species are present. Since Fenimore and Jones (1967) found that every tenth collision between a particle and a hydroxyl radical results in a successful reaction, the rate constant for reaction 12 was calculated from kinetic theory.

Numerical method

The 25 equations used to model the particle forming process consist of a group of nonlinear, coupled, first-order differential equations with time constants (rate constants) that vary by several orders of magnitude. With these characteristics the equations were found to show signs of stiffness. The presence of stiffness was evident when the solution of the equations was unstable (negative concentrations) when implicit methods such as the Runge-Kutta method were used.

The method of Gear (1971) was used to numerically integrate the equations because of the stiffness problem. A double precision IMSL (International Mathematical and Statistical Library) routine called DGEAR was used to solve the differential equations. To use DGEAR, initial conditions, error tolerance, and initial step sizes were specified. The numerical routine calculated the concentration of the chemical and particle species at each time step as the solution progressed. The time steps were incremented by a percentage of the time expired so that each time decade would have the same number of steps. A CPU time of approximately 10 min was necessary to integrate the equations out to 1 s with 10^4 time steps per decade.

Results and Discussion

Gas phase concentrations

The model program was run under various conditions to observe the effect of variables such as temperature and initial reactant concentrations on reactor yield and product properties. The numerical code calculated concentrations of 15 chemical species and 10 particle classes for each time step. An example of the concentration profiles generated by the code appear in Figures 3 through 5. The conditions used in the numerical code for these results were a temperature of 1,800 K and an equivalence ratio (stoichiometric oxygen for complete combustion of benzene divided by available oxygen) of $\phi = 5.5$. The initial gas phase concentrations are shown in Table 3.

Figure 3 shows the concentration profiles of the reactants: benzene and oxygen. The concentrations remain relatively constant for an initial period and then drop off sharply at roughly 1 ms. This behavior is also apparent in Figure 4, which shows the concentration profiles of several of the important intermediate species. In Figure 4, after the radical pool increases to significant concentrations the values also drop abruptly, similar to the profiles of the reactants. Thus, the time scale of the chemical reactions necessary to produce the carbon black precusors for the assumed initial conditions is on the order of 1 ms. This result agrees well with the work of Graham (1975), who found that the time scale of the hydrocarbon-to-particle reactions was 1.0–1.5 ms under similar conditions. Since the carbon black reactor residence times are approximately 10 ms, a period of 1 ms for the initial chemical phase of the model appears to be reasonable.

Finally, Figure 5 shows the concentration profiles for two of the gaseous products produced in the reaction sequence. These products, carbon monoxide and hydrogen, increase to significant concentrations again at approximately 1 ms.

Table 3. Initial Gas Phase Concentration

Component	Conc. mol/L
C_6H_6	3.05×10^{-4}
O_2	4.15×10^{-4}
H_2O	7.86×10^{-4}
CO_2	5.0×10^{-4}
N_2	4.64×10^{-3}

$T = 1{,}800$ K; $\phi = 5.5$

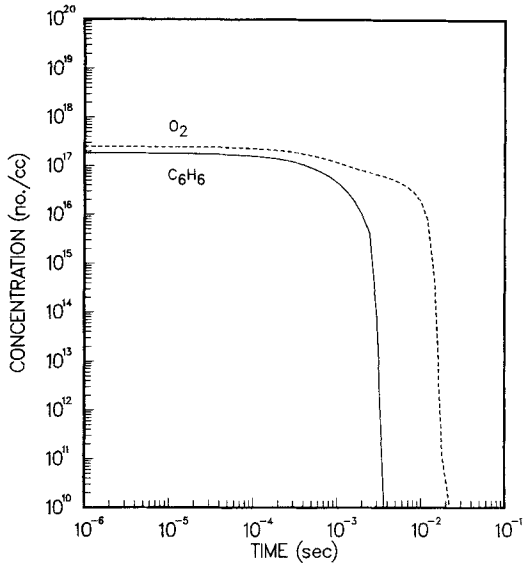

Figure 3. Concentration profiles of initial reactants.
T = 1,800 K; ϕ = 5.5

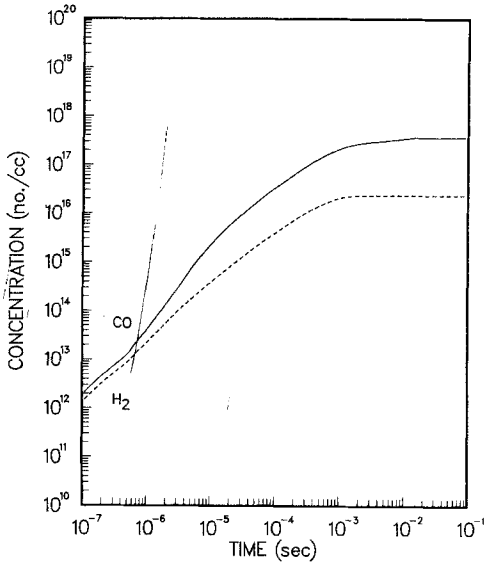

Figure 5. Concentration profiles of products.
T = 1,800 K; ϕ = 5.5

Sensitivity

A sensitivity analysis was performed in order to determine which reactions or rate constants are critical in the gas phase kinetic model of Table 1. This was accomplished by recording the percent change in the maximum concentration of the C_6H_5 intermediate by individually altering the rate constant for each reaction as indicated in Table 4.

It was found that the kinetic scheme of Table 1 was most sensitive to the decomposition of benzene, reaction 1, and to the oxidation of the phenyl radical C_6H_5, reaction 11. Clearly, inaccuracies in either rate constant could significantly alter the availability of particle nuclei. However, while an increase or decrease in the rate constant for the decomposition of benzene resulted in a similar change in the size and concentration of carbon black particles for a fixed reactor residence time, the same conclusion could not be drawn concerning the oxidation of the phenyl radical. In the latter case, significant changes in the phenyl radical pool by reaction 11 were found to have little effect on the amount of carbon black formed since the oxidation of C_6H_5 produced larger concentrations of the growth species C_2H_2 and C_2H_3.

From the sensitivity analysis, reactions 2 and 10 were found to be the next most important. In these reactions, the H radical formed in reaction 1 attacked both of the initial reactants, C_6H_6 and O_2. From the trends shown in Table 4, reaction 10 behaved as an O_2 sink. When more O_2 was used in reaction 10, less O_2 was available to participate in the ring-fracturing reaction of the phenyl radical, reaction 11. On the other hand, reaction 2 acted

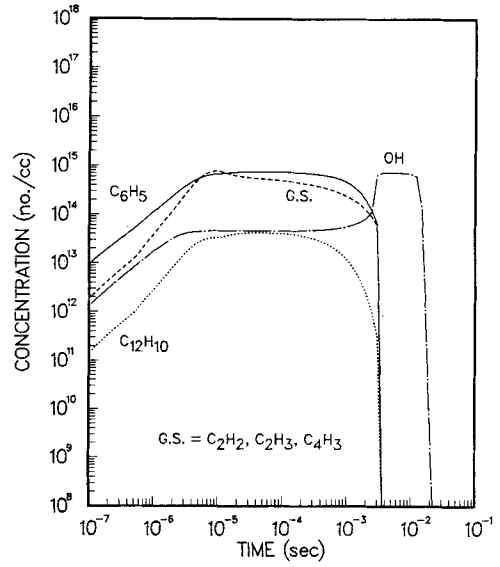

Figure 4. Concentration profiles of key intermediate species.
G.S., growth species; T = 1,800 K; ϕ = 5.5

Table 4. Sensitivity Analysis of Gas Phase Reactions at 1,800 K

Reaction No.*	C_6H_5 Conc., % change	
	$k/2$	$2k$
1	−47	89
2a	12	−12
2b	0	0
3a	−3	5
3b	3	−2
4a	0	0
4b	0	0
5	0	0
6	0	0
7	0	0
8	0	0
9	0	0
10	−13	15
11	93	−48
12	0	0

*See Table 1

as an H radical sink, leaving fewer H radicals to participate in reaction 10. This led to an increase in available O_2 and thus an increase in the phenyl radical consumption of reaction 11.

From Table 4 the remaining reactions, 2 through 9 in Table 1, were found to have little effect on the concentration of the initial nucleating species C_6H_5. Although these remaining reactions involving the production and consumption of the biphenal radical $C_{12}H_{10}$ and the oxidation of benzene could be important at other temperatures or equivalence ratios, they may be neglected under the conditions of the present study.

Particle evolution

Carbon black particles consist of primary nodules clustered together in a chainlike formation that looks like a string of pearls. In the present code all particles are assumed to be spherical equivalents of these clusters, with a spherical equivalent diameter used to calculate the collision frequencies between various particles. Figure 6 shows the concentration profiles of the individual particle classes. The smallest particle class develops rapidly. At approximately 1 ms, after the initial chemical phase, the concentrations of particles in the smaller size classes decrease. This depletion is caused by a decrease in the rate of formation in the number of initial particles and the loss of smaller particles by coagulation. Also, oxidation of the smaller particles contributes to their depletion. It is also apparent in Figure 6 that after 10 ms most of the carbon particles are in the F, G, or H class as listed in Table 2. This corresponds to the reactor residence time. Thus, if carbon black aggregates are composed of spherical units of roughly 35 nm dia., there are approximately 1, 6, or 50 units per aggregate in the most popular size classes, F, G, H, respectively. Moreover, there are few particles in the largest classes, I and J, at the reactor exit, as indicated in Fig. 6.

Because particles are initially absent in the reaction zone, the particle distributions are formed as the particles form, grow, and coagulate. Figure 7 shows the development of the particle distributions on a log probability plot when the model is run at a temperature of 1,800 K. For times greater than 3 ms, a self-preserving log normal distribution of the various particle sizes develops,

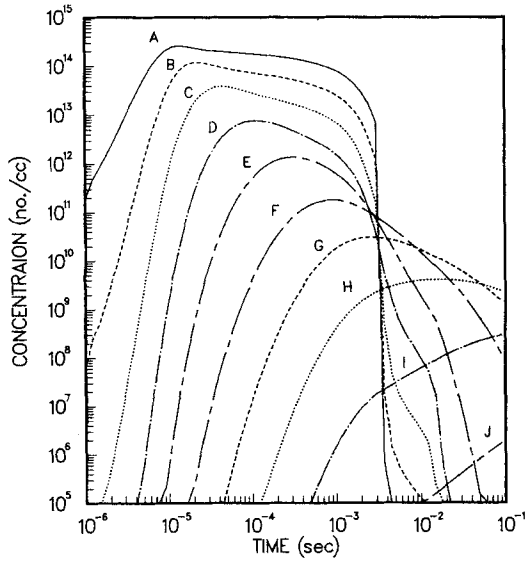

Figure 6. Concentration profiles of particle classes A–J.
T = 1,800 K; ϕ = 5.5

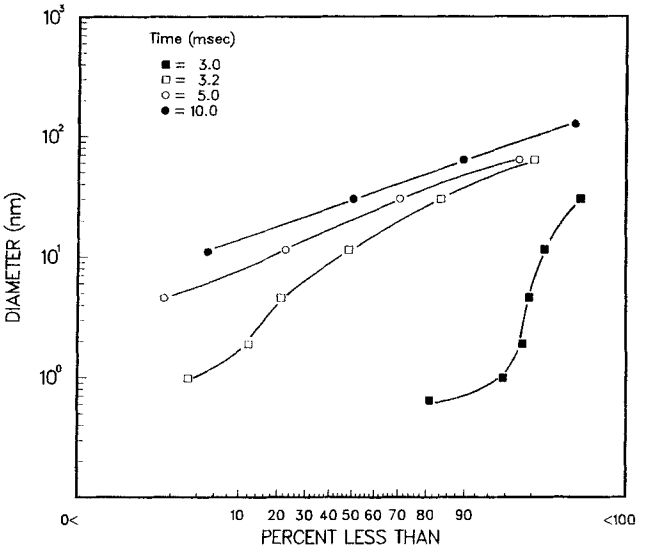

Figure 7. Particle count distribution at various times on log normal axes.
T = 1,800 K; ϕ = 5.5; data points are numerical computations

as evidenced by the linearity of the particle distribution when plotted on log probability axes. This is not the case for times less than 3 ms, since the log normal distribution has not yet developed, as indicated in Figure 7 by the nonlinear data.

The concentration profiles at 2,000 and 1,600 K were similar to those at 1,800 K except for a variation in time scales. At 1,600 K the benzene feed did not become depleted until 50 ms, as shown in Figure 8. However, at 2,000 K benzene was depleted at 0.5 ms. Thus, the effect of temperature on the reactions displayed an exponential (Arrhenius) effect. Clearly, if the residence time in the carbon black reactor is 10 ms, the temperature must be above roughly 1,700 K for complete consumption of the benzene feed stock and the production of carbon black particles.

The mass average diameter of the carbon black particles was determined with the present model as a function of time within the reactor for temperatures of 1,600, 1,800, and 2,000 K as indicated in Figure 9. It is apparent that the mass average diameter of the carbon particles increases at a rate corresponding to a

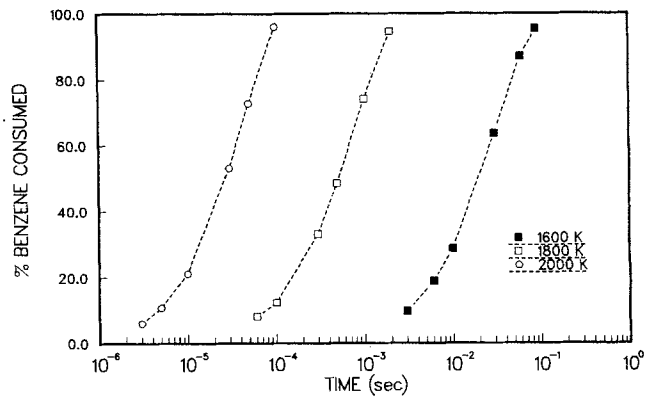

Figure 8. Percent benzene reacted vs. time at several temperatures.
ϕ = 5.5; data points are numerical computations

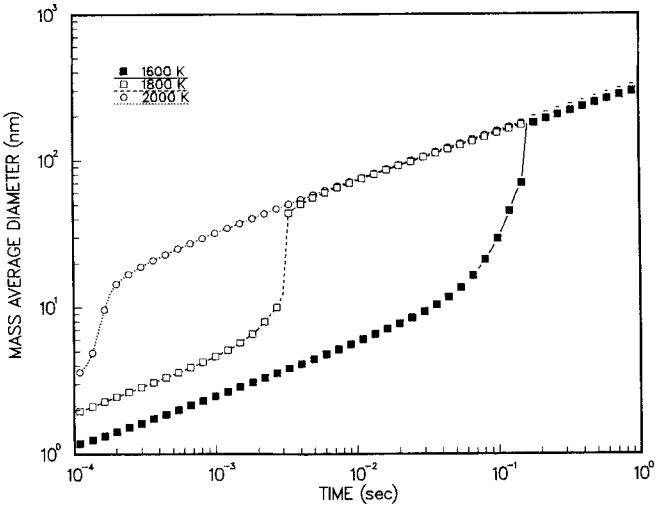

Figure 9. Mass average particle diameter vs. time.
ϕ = 5.5; data points are numerical computations

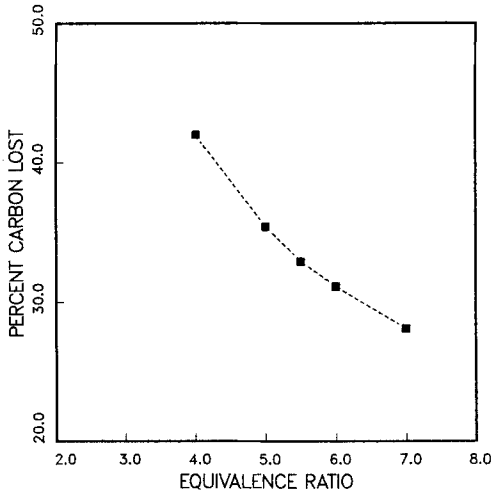

Figure 10. Percent feed carbon in benzene lost to CO at t = 10 ms vs. equivalence ratio.
T = 1,800 K; data points are numerical computations

self-preserving log normal distribution after the benzene feed stock has been depleted. As also noted in Figure 7, the carbon particle distribution appears to have reached the log normal stage in Figure 9 at a reactor residence time of 10 ms, for a reactor temperature of 1,800 K.

Effects of temperature and equivalence ratio

The effects of temperature and equivalence ratio on the model results follow the same general trends that are observed in normal reactor operations. Figure 8 shows the effect of temperature variation on the model results. At higher temperatures the initial benzene charge is consumed faster. The increased reaction rates result from the temperature dependence of the rate constants of the chemical reactions and the coagulation constants of the particle interactions. In the operation of a carbon black reactor, temperature affects the residence time of the particles within the reactor. Higher temperatures cause the gases within the reactor to expand, resulting in larger throughput velocities that lower the particle residence time within the reactor.

One way of controlling the temperature within a carbon black reactor is to vary the equivalence ratio ϕ. By decreasing the equivalence ratio, more oxygen is available in the reaction zone to promote the exothermic oxidation reactions, which increases the temperature in the reactor. One drawback to using low equivalence ratios in the reactor, however, is the production of large amounts of oxidation products (e.g., carbon monoxide) instead of the pyrolytic products (i.e., carbon particles).

Figure 10 shows the amount of the initial carbon found in the benzene feedstock lost to carbon monoxide production at various equivalence ratios. As the equivalence ratio ϕ increases, less of the carbon in the feedstock forms carbon black per pound of benzene feedstock. The model predicts that 33% of the initial carbon benzene found in the feedstock forms carbon monoxide at an equivalence ratio of ϕ = 5.5. From experiments run on an actual reactor, 40% of the initial carbon was converted into carbon monoxide at the same equivalence ratio. The difference in these values may result from errors in the rate constants of the reaction scheme used in the present model. Another possible explanation is that another oxidating species, such as the oxygen radical, is participating in the burnout mechanism. This would result in the oxidation of soot particles and the formation of additional carbon monoxide.

Comparison of experimental and model results

Twenty experimental runs were performed on a pilot plant scale reactor at the Phillips Research Center in Bartlesville, Oklahoma. In these experiments benzene vapor was fed to a reactor with a reaction temperature of 1,800 K and an equivalence ratio of ϕ = 5.5. The residence time in the reactor was 10 ms, at which time a water spray was introduced to quench the reactions. Gas and carbon samples were collected at the reactor exit and analyzed. The mass average diameter of the carbon particles was then determined from two adsorption tests performed on the carbon samples using a correlation developed by Janzen (1982):

1. CTAB (hexadecyltrimethyl-ammonium bromide) adsorption to determine external surface area
2. DBP (dibutyl phthalate) adsorption to determine void volume

A comparison of the experimental and model results appears in Table 5.

From Table 5, the largest difference between the experimental and model values occurs in the particle concentrations at the reactor exit. For example, it was found that the present model predicts a mass average carbon particle diameter of 73 nm, which is just 10% larger than the average from the experimental data but within their scatter. However, the numerical model underestimates the particle concentration by 18%. These differences may be attributed to the errors in the nucleation kinetics

Table 5. Experimental and Model Results at 10 ms

	Exp.	Model
Mass avg. particle dia., nm	66 ±10	73
Geometric std. dev.	—	1.7
Particle conc., no./cm^3	4.5 ±0.6 × 10^{10}	3.7 × 10^{10}
CO conc., mol/L	7.9 ±0.5 × 10^{-4}	6.0 × 10^{-4}

T = 1,800 K; ϕ = 5.5

of the phenyl radical. Possibly, some phenyl radicals are lost by other oxidation or ring-fracturing mechanisms that would result in the formation of fewer carbon particles. These numerical results, however, are within the error bounds of the simplified kinetics and coagulation parameters used in the present model.

The other values in Table 5 that deviate noticeably are the carbon monoxide concentrations. The CO concentration calculated in the model underestimates the experimental value by 24%. As stated above, this underestimation could be caused by another oxidizing species, such as an oxygen radical.

Conclusions

From the results obtained, the numerical model closely approximates the synthesis of carbon black from benzene. Though some discrepancies do occur between the numerical results and the actual reactor data, the present simple model appears to simulate the basic steps in carbon black formation.

From the model results at 1,800 K, concentration profiles of the gaseous reactants and products indicate reaction time scales on the order of 1 ms. This time scale is appropriate since reactor residence times at 1,800 K are on the order of 10 ms and the additional time in the reactor is necessary for particle growth and coagulation.

From initially empty particle classes, a log normal distribution of particles develops and is maintained as the particles grow and coagulate. When the sizes of the particles were compared with experimental values, good agreement was obtained.

The effect of temperature and equivalence ratio on the model results follow the trends observed in normal reactor operation. Higher temperatures result in faster reaction times while lower equivalence ratios are shown to decrease the carbon black production due to increased oxidation of the benzene feedstock.

Acknowledgment

The authors wish to acknowledge the financial support of the Phillips Research Center in Bartlesville, Oklahoma. Additional support was provided by a President's Graduate Fellowship to J. J. Ivie from the Georgia Institute of Technology. The authors benefited from technical discussions with Paul J. Cheng of the Phillips Research Center concerning carbon black production.

Notation

A = preexponential coefficient in the rate constant, $cm^3/mol \cdot s$ or $1/s$
C_i = mean thermal velocity of particle i, m/s
D_i = diffusion coefficient of particle i, m^2/s
E = activation energy, kJ
fxy = coagulation rate constant for particles in size classes x and y, m^3/s
g_i = function of particle radius and mean free path for particle i
$g_{ij} = (g_i^2 + g_j^2)^{1/2}$
GS = growth species, C_2H_2, C_4H_3, C_2H_3
G_i = growth species, C_2H_2, C_2H_3, or C_4H_3
kx = rate constant for chemical reaction x, $L/mol \cdot s$ or $1/s$
l_i = mean free path of particle i, m
n = stoichiometric coefficient
N_i = nucleating species, C_6H_5 or $C_{12}H_{10}$
Px = carbon particle containing x carbon atoms or in the x size class
r_i = radius of particle i, m
t = time, s
T = temperature, K
ϕ = equivalence ratio, stoichiometric to available O_2
[ ] = concentration of species within brackets, mol/L
i, j, x, y, z = subscripts

Literature Cited

Abrahamson, J., "Saturated Platelets Are New Intermediates in Hydrocarbon Pyrolysis and Carbon Formation," *Nature*, **266**, 323 (1977).
Donnet, J. and A. Voet, *Carbon Black: Physics, Chemistry and Elastomer Reinforcement*, Marcel Dekker, New York (1976).
Fenimore, C. P., and G. W. Jones, "Oxidation of Soot by OH Radicals," *J. Phys. Chem.*, **71**, 593 (1967).
Frenklach, M., and J. Warnatz, "Detailed Modeling of PAH Profiles in Sooting Low-Pressure Acetylene Flame," *Combust. Sci. Tech.*, **51**, 265 (1987).
Fuchs, N. A., *Mechanics of Aerosols*, Pergamon, New York (1964).
Fujii, N., and T. Asaba, "High-Temperature Reaction of Benzene," *J. Fac. Eng., Univ. Tokyo*, **34**, 189 (1977).
Gear, C. W., "The Automatic Integration of Ordinary Differential Equations," *Comm. ACM*, **14**, 176 (1971).
Gelbard, F., Y. Tambour, and J. H. Seinfeld, "Sectional Representations for Simulation Aerosol Dynamics," *J. Coll. Interface Sci.*, **76**, 541 (1980).
Graham, S. C., J. B. Homer, and P. L. T. Rosenfeld, "The Formation and Coagulation of Soot Aerosols Generated by the Pyrolysis of Aromatic Hydrocarbons," *Proc. Roy Soc. A*, **344**, 259 (1975).
Haynes, B. S., and G. Wagner, "Soot Formation," *Prog. Energy Combust. Sci.*, **7**, 229 (1981).
Howard, J. B., and J. D. Bittner, "Preparticle Chemistry in Soot Formation," *General Motors Symp. on Soot Formation*, 109 (1980).
Hsu, D. S. Y., C. Y. Lin, and M. C. Lin, "CO Formation in the Early Stage High-Temperature Benzene Oxidation under Fuel Lean Conditions: Kinetics of the Initiation Reaction, $C_6H_6 \rightarrow C_6H_5 + H$," *20th Symp. (Int.) Combust.*, Combustion Inst., Pittsburg, 623 (1984).
Janzen, J., "Physiochemical Characteristics of Carbon Black," *Rubber Chem. Tech.*, **55**, 669 (1982).
Jensen, D. E., "Prediction of Soot Formation Rates: A New Approach," *Proc. Roy. Soc. A*, **338**, 375 (1974).
Kiefer, J. H., L. J. Mizerka, M. R. Patel, and H. C. Wei, "A Shock Tube Investigation of the Major Pathways in High-Temperature Pyrolysis of Benzene," *J. Phys. Chem.*, **89**, 2013 (1985).
Lahaye, J., and G. Prado, "Mechanisms of Carbon Black Formation," *Chem. Phys. Carbon*, **14**, 168 (1978).
Madronich, S., and W. Felder, "Kinetics and Mechanism of the Reaction of OH with C_6H_6 over 790–1,410 K," *J. Phys. Chem.*, **89**, 3556 (1985).
Medalia, A. I., "Morphology of Aggregates. I," *J. Coll. Interface Sci.*, **24**, 393 (1967).
———, "Morphology of Aggregates. VI," *J. Coll. Interface Sci.*, **32**, 115 (1970).
Palmer, H. B., and C. F. Cullis, "The Formation of Carbon from Gases," *Chem. Phys. Carbon*, **1**, 265 (1965).
Seigneur, C., A. B. Hudischewskyi, J. H. Seinfeld, K. T. Whitby, E. R. Whitby, J. R. Brock, and H. M. Barnes, "Simulation of Aerosol Dynamics: A Comparative Review of Mathematical Models," *Aerosol Sci. Tech.*, **5**, 205 (1986).
Singh, H. J., and R. D. Kern, "Pyrolysis of Benzene behind Reflected Shock Waves," *Combust. Flame*, **54**, 49 (1983).

Manuscript received Dec. 29, 1987, and revision received June 13, 1988.